Approximations to the scattering of water waves by steep topography

By R. PORTER[1] **AND D. PORTER**[2]

[1]School of Mathematics, University of Bristol, Bristol, BS8 1TW, UK
[2]Department of Mathematics, University of Reading, PO Box 220, Whiteknights,
Reading, RG6 6AX, UK

A new method is developed for approximating the scattering of linear surface gravity waves on water of varying quiescent depth in two dimensions. A conformal mapping of the fluid domain onto a uniform rectangular strip transforms steep and discontinuous bed profiles into relatively slowly varying, smooth functions in the transformed free-surface condition. By analogy with the mild-slope approach used extensively in unmapped domains, an approximate solution of the transformed problem is sought in the form of a modulated propagating wave which is determined by solving a second-order ordinary differential equation. This can be achieved numerically, but an analytic solution in the form of a rapidly convergent infinite series is also derived and provides simple explicit formulae for the scattered wave amplitudes. Small-amplitude and slow variations in the bedform that are excluded from the mapping procedure are incorporated in the approximation by a straightforward extension of the theory. The error incurred in using the method is established by means of a rigorous numerical investigation and it is found that remarkably accurate estimates of the scattered wave amplitudes are given for a wide range of bedforms and frequencies.

1. Introduction

A variety of methods has been developed in recent years to determine the scattering of linear surface water waves over undulating beds in two dimensions. If the undulations are of small amplitude or slowly varying, accurate estimates of the scattered wave amplitudes are provided by the relatively simple approximations of the 'mild-slope' type. A recent entry into an extensive literature in this area is provided by Porter (2003). For undulations that are not restricted in this way, however, considerably more effort is required to resolve the scattering process to the extent that the methods that have been devised are generally targeted at providing accurate solutions by computational means. We will give examples of these methods later.

The aim of the present work is to develop an approximation technique for any bed shape that has the simplicity of the mild-slope approach, whilst retaining a level of accuracy that is adequate for most practical purposes.

The essential difficulty in the problem is the application of a Neumann condition, representing zero normal flow, on a bed profile of a general shape. By conformally mapping the fluid domain into a strip of uniform width in such a way that the bed profile transforms to a coordinate line, this difficulty is removed and the bed condition can now easily be satisfied exactly. Although the transformation process complicates

the usual mixed boundary condition at the free surface by introducing a variable coefficient there, the effect of steep and even discontinuous bedforms is distributed across a comparatively wide interval in the revised free-surface condition.

The idea of using conformal mappings in this way is not new and was implemented by Fitz-Gerald (1976), who devised integral equation techniques to solve the resulting potential problem in the transformed plane. Shortly afterwards Hamilton (1977) used the mapping technique to develop a nonlinear formulation of the problem whose long-wave limit results from the zeroth-order approximation to the solution. Both Fitz-Gerald (1976) and Hamilton (1977) presented several families of mappings which both demonstrate that the method can be applied to a wide range of bedforms and illustrate the property that a rapidly varying bed shape is transformed into a relatively slowly varying free-surface condition.

Evans & Linton (1994) took advantage of this property by using a piecewise-constant approximation of the transformed free-surface condition in conjunction with the exact solution of Weitz & Keller (1950), derived for the case in which there is a single jump between two constant free-surface states. Evans & Linton obtained impressive results for the scattered wave amplitudes by comparison with those obtained using other methods, in a number of test problems and for a selection of parameter values.

Our approach is different from those of Fitz-Gerald (1976), Hamilton (1977) and Evans & Linton (1994). We exploit the fact that large gradients in the bed shape are mapped to smaller gradients in the free-surface condition by assuming the latter to be sufficiently slowly varying that an approximation of the 'mild-slope' variety can be applied. Thus, at each horizontal location the vertical dependence is imposed on the solution that corresponds to a propagating wave at the local version of the free-surface condition. The effect of this approximation is therefore to seek a propagating wave solution that is modulated by the variations in the free-surface condition. To implement it we use a variational principle in the spirit of the Rayleigh–Ritz method and this process both removes the vertical coordinate from the proceedings and has a 'smoothing' effect. We therefore obtain a vertically averaged approximation which is completed by solving a second-order ordinary differential equation and this can be achieved numerically. However, we also develop an analytic solution in the form of an infinite series, by using an integral equation method, with the ultimate aim of giving simple explicit formulae for the amplitudes of the scattered waves.

Despite the range of mappings developed by Fitz-Gerald (1976), not all bedforms can be dealt with in this way, of course, and we therefore extend the technique to encompass a larger class of profiles. We therefore envisage a bedform consisting of steep components, which can be mapped into a uniform strip, and slow variations about this which distort the transformed domain and appear in the transformed bed condition. The method already described may be carried over with an adjustment to deal with the revised bed condition. Again the problem is reduced to an ordinary differential equation, which now includes as a special case the conventional mild-slope equation derived originally by Smith & Sprinks (1975) and Berkhoff (1976) and in its extended form by Chamberlain & Porter (1995). The significance of a judicious choice of scaling, which led to the recent simplified version of the mild-slope equation identified by Porter (2003), is transparent in the present development.

Our objective is to obtain a simple approximation for a wide range of bedforms and wave frequencies and not to derive the exact solution. If the latter is required, existing methods may be used without introducing the complication of the mapping procedure. These include the integral equation method of Porter & Porter (2000),

the multi-mode extension of the mild-slope equation developed in a succession of papers including those by Massel (1993), Porter & Staziker (1995), Athanassoulis & Belibassakis (1999) and Chamberlain & Porter (2006), and discretization methods such as the finite element and boundary integral techniques, the essential features of which can be found in Mei (1983). Each of these requires sophisticated numerical algorithms and considerable computational effort. For this reason we do not pursue the multi-mode version of the current approach, which is easily formulated but can only reproduce results that are already available using established methods.

One requirement of the present work, therefore, is a thorough investigation of the error incurred by the method and we are able to carry this out by reference to particular bedforms. Especially useful in this context is a profile for which there is both a conformal mapping and an exact solution, identified by Roseau (1976) and extended using a different approach by Evans (1985).

The plan is to formulate the problem in the physical and transformed plane in §2, considering at this stage only bedforms that map onto a strip of uniform width. The approximation is developed for this case in §3, together with the derivation of the analytic solution, a description of the numerical solution method and a set of examples, including a rigorous error estimate based on numerical experiments. In §4 the extension of the theory is given to the case in which the bedform varies about a profile that can be mapped conformally, with a further example.

2. Formulation

We are concerned with two-dimensional scattering and use Cartesian coordinates x, y, arranged so that y is measured vertically upwards from the undisturbed free surface. The bed is given by $y = -h(x)$ for $-\infty < x < \infty$, where the function h is such that

$$h(x) \to \begin{cases} h(-\infty) = h_0, & x \to -\infty, \\ h(\infty) = h_1, & x \to \infty, \end{cases} \qquad (2.1)$$

h_0 and h_1 being constants.

According to linear wave theory, the motion is described by the velocity potential

$$\Phi(x, y, t) = \mathrm{Re}\{\phi(x, y)\mathrm{e}^{-\mathrm{i}\omega t}\},$$

where ϕ satisfies

$$\left. \begin{aligned} &\phi_{xx} + \phi_{yy} = 0, \quad (x, y) \in D := \{-\infty < x < \infty, -h(x) < y < 0\}, \\ &\phi_n \equiv \phi_z + h'(x)\phi_x = 0, \quad -\infty < x < \infty, \ y = -h(x), \\ &\phi_y - K\phi = 0, \quad -\infty < x < \infty, \ y = 0, \end{aligned} \right\} \qquad (2.2)$$

in which ϕ_n denotes the normal derivative on $y = -h(x)$ and $K = \omega^2/g$. It has been assumed here that $h(x)$ is single-valued and differentiable. However, we will later present results for bed shapes where these assumptions are violated and in these cases D denotes the domain occupied by the fluid and the bed condition is just $\phi_n = 0$. The reason for setting the problem in the form (2.2) is that it connects directly with theory developed later.

If we define k_0 and k_1 by

$$K = k_i \tanh(k_i h_i), \quad i = 0, 1,$$

then the far-field behaviour of ϕ can be determined by separation of variables in (2.2) and we choose

$$\phi(x, y) \sim \begin{cases} \{A_0 e^{ik_0 x} + B_0 e^{-ik_0 x}\} \, c(k_0 h_0) \cosh k_0(y + h_0), & x \to -\infty, \\ \{A_1 e^{-ik_1 x} + B_1 e^{ik_1 x}\} \, c(k_1 h_1) \cosh k_1(y + h_1), & x \to \infty, \end{cases} \tag{2.3}$$

in which A_0 and A_1 are the given amplitudes of incident waves and the complex amplitudes B_0 and B_1 of the scattered waves are to be found. The normalizing factors are taken to be

$$c(k_i h_i) = \left\{ h_i^{-1} \int_{-h_i}^{0} \cosh^2 k_i(y + h_i) \, \mathrm{d}y \right\}^{-1/2}.$$

The scattering process can be summarized through the matrix $\mathscr{S}$, defined by

$$\begin{pmatrix} B_0 \\ B_1 \end{pmatrix} = \mathscr{S} \begin{pmatrix} A_0 \\ A_1 \end{pmatrix}, \quad \mathscr{S} = \begin{pmatrix} R_0 & T_1 \\ T_0 & R_1 \end{pmatrix}, \tag{2.4}$$

R_i and T_i being the respective reflection and transmission coefficients. Porter & Chamberlain (1997) provided a simple proof that

$$\mathscr{S} \overline{\mathscr{S}} = I, \tag{2.5}$$

leading to well-known identities due originally to Kreisel (1949).

We now follow Fitz-Gerald (1976) and Evans & Linton (1994) by mapping the domain D into a domain $\mathscr{D}$ of constant height in the (ξ, η)-plane by means of the conformal transformation $z = F(\zeta)$, where $z = x + \mathrm{i}y$ and $\zeta = \xi + \mathrm{i}\eta$. In fact we choose $\mathscr{D} := \{-\infty < \xi < \infty, -1 < \eta < 0\}$ and arrange that $y = 0$ transforms to $\eta = 0$. The boundary value problem (2.2) therefore becomes

$$\left.\begin{aligned} \varphi_{\xi\xi} + \varphi_{\eta\eta} &= 0, && -\infty < \xi < \infty, \ -1 < \eta < 0, \\ \varphi_\eta &= 0, && -\infty < \xi < \infty, \ \eta = -1, \\ \varphi_\eta - f(\xi)\varphi &= 0, && -\infty < \xi < \infty, \ \eta = 0, \end{aligned}\right\} \tag{2.6}$$

in which $\varphi(\xi, \eta) = \phi(x, y)$ and $f(\xi) = K F'(\xi)$ is real-valued, positive and continuous. As indicated already, the main obstacle to progress in (2.2), the condition on the bed, has been simplified in (2.6) to the extent that it is easy to satisfy it exactly.

The mapping function must be such that $F(\zeta) \to h(\pm\infty)\zeta$ as $\xi \to \pm\infty$, so that

$$f(\xi) \to \begin{cases} f_0 \equiv K h_0, & \xi \to -\infty, \\ f_1 \equiv K h_1, & \xi \to \infty. \end{cases} \tag{2.7}$$

Therefore (2.3) corresponds to

$$\varphi(\xi, \eta) \sim \begin{cases} \{A_0 e^{i\kappa_0 \xi} + B_0 e^{-i\kappa_0 \xi}\} \, c(\kappa_0) \cosh \kappa_0(\eta + 1), & \xi \to -\infty, \\ \{A_1 e^{-i\kappa_1 \xi} + B_1 e^{i\kappa_1 \xi}\} \, c(\kappa_1) \cosh \kappa_1(\eta + 1), & \xi \to \infty, \end{cases} \tag{2.8}$$

where $\kappa_i = k_i h_i$ is the positive real root of $f_i = \kappa_i \tanh \kappa_i$ and

$$c(\kappa) = \left\{ \int_{-1}^{0} \cosh^2 \kappa(\eta + 1) \, \mathrm{d}\eta \right\}^{-1/2} = 2\{\kappa/(2\kappa + \sinh 2\kappa)\}^{1/2}.$$

In all of the examples given later the condition (2.7) is satisfied because

$$f(\xi) = f(\pm\infty) + O(e^{-\delta_\pm |\xi|}), \quad \xi \to \pm\infty, \tag{2.9}$$

where $\delta_\pm > 0$, and we therefore assume that this property holds in general.

The boundary-value problem consisting of (2.6) and (2.8) can be formulated as an integral equation (if $h_0 = h_1$) or a system of coupled integral equations (if $h_0 \neq h_1$) and solved numerically, the approach being similar to that of Porter & Porter (2000). Fitz-Gerald (1976) adopted a related strategy by deriving an integro-differential equation that led to numerical results. Evans & Linton (1994), however, took advantage of the fact that the function f occurring in the transformed problem (2.6) varies relatively slowly, even for rapid variations in the bed shape, and replaced it with a piecewise-constant function to produce good approximations.

Our present approach is to suppose that f is slowly varying and to approximate the solution of (2.6) and (2.8) in such a way as to provide relatively simple estimates of the components of the scattering matrix $\mathscr{S}$.

3. An approximation

The approximate solution of (2.6) is generated by using an equivalent variational principle in conjunction with the Rayleigh–Ritz method. One aim of the approximation is to remove the η dependence from the process by postulating the form of φ in a particular way and for the immediate purpose we can consider the problem on an arbitrary finite domain with $a < \xi < b$, say. This avoids the need to form a functional that is consistent with the radiation conditions and converges on the infinite domain. The radiation conditions will be applied to the resulting approximation in due course.

We therefore let

$$L(\psi) = \frac{1}{2} \int_a^b \left\{ \int_{-1}^0 (\psi_\xi^2 + \psi_\eta^2)\, \mathrm{d}\eta - f(\xi)(\psi^2)_{\eta=0} \right\} \mathrm{d}\xi. \tag{3.1}$$

The first variation of L is

$$\delta L = \int_a^b \left\{ ((\psi_\eta - f(\xi)\psi)\delta\psi)_{\eta=0} - (\psi_\eta \delta\psi)_{\eta=-1} - \int_{-1}^0 (\psi_{\xi\xi} + \psi_{\eta\eta})\delta\psi\, \mathrm{d}\eta \right\} \mathrm{d}\xi$$
$$+ \left[\int_{-1}^0 \psi_\xi \delta\psi\, \mathrm{d}\eta \right]_{\xi=a}^{\xi=b}. \tag{3.2}$$

As we are not at present concerned with the conditions on the lateral boundaries, we may choose $\delta\psi = 0$ at $\xi = a$ and $\xi = b$ for $-1 \leqslant \eta \leqslant 0$, and it then follows that L is stationary at $\psi = \varphi$ if and only if φ satisfies equations (2.6) for $a < \xi < b$. Therefore, finding the stationary point of L is equivalent to finding a solution of (2.6) and an approximation to the stationary point is an approximation to a solution.

We base our approximation on the solution of (2.6) with $f = f_i$, where f_i is constant. In this case the normalized eigenfunction of the boundary-value problem associated with propagating waves having wavenumber κ_i is

$$v_i(\eta) = c(\kappa_i) \cosh \kappa_i(\eta + 1), \tag{3.3}$$

where κ_i now denotes the positive real root of

$$f_i = \kappa \tanh \kappa \tag{3.4}$$

for any value of f_i. This extends the notation has already been used in (2.8) in relation to the far-field values of f. It is convenient to express the normalization by using the

inner product

$$(u, v) = \int_{-1}^{0} u\bar{v}, \quad ||u||^2 = (u, u), \qquad (3.5)$$

in terms of which $||v_i|| = 1$.

The simplest approximation that makes use of the solution for a constant fluid depth is the modulated propagating wave based on (3.3) and (3.4) and given by

$$\varphi(\xi, \eta) \approx \psi(\xi, \eta) = \chi(\xi)v(\xi, \eta), \quad v(\xi, \eta) = c(\kappa(\xi)) \cosh \kappa(\xi)(\eta + 1), \qquad (3.6)$$

in which $\kappa(\xi)$ is the positive real root of

$$f(\xi) = \kappa(\xi) \tanh \kappa(\xi). \qquad (3.7)$$

The dependence of ψ on η is therefore approximated by the eigenfunction v at each value of f. The approximation may be regarded as a continuous counterpart of the discretization used by Evans & Linton (1994). They replaced f by a finite sequence of constant values f_i and, for each f_i, considered only the propagating wave contributions. However, by using the solution of Weitz & Keller (1950), Evans & Linton did incorporate the effect of evanescent modes across the junctions between two different values of f and this contrasts with the exclusion of decaying modes from the present approximation. The structure of (3.6) is analogous to that leading to the modified mild-slope equation of Chamberlain & Porter (1995), which is developed from the original problem (2.2) under the restrictive condition that the depth h is slowly varying. Here we assume that f is slowly varying, in the sense that $|f'| \ll \kappa f$ for all ξ, and our expectation, which is realized in the examples given later, is that the 'stretching effect' of the transformation will allow the present approximation to be applied to steep bed profiles, despite its simple form.

A differential equation for the function χ in (3.6) follows by making L stationary with respect to arbitrary variations $\delta\chi$ that vanish at $\xi = a$ and $\xi = b$. As the approximation ψ satisfies the exact boundary conditions on $\eta = 0$ and $\eta = -1$, we see from (3.2) that

$$\delta L = -\int_{a}^{b} \delta\chi \int_{-1}^{0} \{(\chi v)_{\xi\xi} + (\chi v)_{\eta\eta}\} v \, d\eta$$

and therefore the differential equation implied by $\delta L = 0$ is

$$\int_{-1}^{0} \{(\chi v)_{\xi\xi} + (\chi v)_{\eta\eta}\} v \, d\eta = 0.$$

Using the fact that $v_{\eta\eta} = \kappa^2 v$ and rearranging, we find that

$$(||v||^2 \chi')' + \{||v||^2 \kappa^2 + (v, v_{\xi\xi})\} \chi = 0,$$

in the notation of (3.5). Now $||v|| = 1$, from which successive differentiations give $(v, v_\xi) = 0$ and $(v, v_{\xi\xi}) = -||v_\xi||^2$. Therefore χ satisfies

$$\chi'' + \{\kappa^2 - ||v_\xi||^2\} \chi = 0, \qquad (3.8)$$

which holds for $|\xi| < \infty$.

An alternative form of (3.8) follows by writing

$$v(\xi, \eta) = ||w||^{-1} w, \quad w = w(f, \eta) = \cosh \kappa(\eta + 1). \qquad (3.9)$$

This notation makes use of (3.7) to define $\kappa = \kappa(f)$ and it is easily shown that

$$\kappa_f = (\cosh(2\kappa) + 1)(\sinh(2\kappa) + 2\kappa)^{-1}. \qquad (3.10)$$

Since $||w||\,||w||_f = (w, w_f)$ then

$$v_\xi = \{||w||^{-1}w\}_f\, f' = \{||w||^{-1}w_f - ||w||^{-3}(w, w_f)w\}f', \tag{3.11}$$

where $f' = \mathrm{d}f/\mathrm{d}\xi$, and therefore (3.8) can be written as

$$\chi'' + \{\kappa^2 - C_0(f)f'^2\}\chi = 0, \tag{3.12}$$

in which

$$C_0(f) = ||w||^{-4}\{||w||^2||w_f||^2 - (w, w_f)^2\}. \tag{3.13}$$

Now the counterparts of w that are associated with evanescent waves in the case of constant f are $w^{(n)} = \cos\kappa^{(n)}(\eta + 1)$ for $n \in I\!N$, where $\kappa^{(n)}$ denote the real positive roots of $f = -\kappa\tan\kappa$. The functions $w, w^{(1)}, w^{(2)}, \ldots$ are orthogonal and form a complete set, and since $(v_\xi, w) = 0$ follows from (3.11), v_ξ can be expressed solely in terms of $w^{(1)}, w^{(2)}, \ldots$. Therefore $||v_\xi||^2 = C_0(f)f'^2$ can be regarded as a correction term that compensates for the omission from the approximation of the eigenfunctions $w^{(n)}$ related to evanescent waves.

For the purpose of applications, we need to evaluate $C_0(f)$ explicitly. Clearly, $||w|| = c^{-1}(\kappa)$ by construction and $w_f = \kappa_f(\eta + 1)\sinh\kappa(\eta + 1)$. Straightforward calculations then give

$$8\kappa^2(w, w_f) = \kappa_f\{2\kappa\cosh(2\kappa) - \sinh(2\kappa)\},$$
$$8\kappa^3||w_f||^2 = \kappa_f^2\{2\kappa^2\sinh(2\kappa) - 2\kappa\cosh(2\kappa) + \sinh(2\kappa) - (4/3)\kappa^3\}$$

and we can use these together with (3.10) to evaluate the coefficient C_0 in (3.12). We thereby arrive at the expression

$$C_0(f) = \frac{(\cosh r + 1)^2}{(\sinh r + r)^4}\left\{\frac{\sinh^2 r}{r^2} + 2\frac{\sinh r}{r} - (2\cosh r + 1) + \frac{2}{3}r\sinh r - \frac{1}{3}r^2\right\},$$

in which $r = 2\kappa$ is an abbreviation.

It follows from (2.9) and (3.7) that

$$f'(\xi) \sim O\left(\mathrm{e}^{-\delta_\pm|\xi|}\right), \quad \kappa'(\xi) \sim O\left(\mathrm{e}^{-\delta_\pm|\xi|}\right), \quad |\xi| \to \infty. \tag{3.14}$$

Therefore (3.12) makes it explicit that the second term in the coefficient of χ does not contribute in the far field. As we would expect, the approximation (3.6) has the exact far-field behaviour and we take

$$\chi(\xi) \sim \begin{cases} A_0\mathrm{e}^{i\kappa_0\xi} + B_0\mathrm{e}^{-i\kappa_0\xi}, & \xi \to -\infty, \\ A_1\mathrm{e}^{-i\kappa_1\xi} + B_1\mathrm{e}^{i\kappa_1\xi}, & \xi \to \infty, \end{cases} \tag{3.15}$$

which is consistent with (2.8).

We can rewrite (3.12) wholly in terms of κ as

$$\chi'' + \kappa^2\{1 - D_0(\kappa)\kappa'^2\}\chi = 0, \quad D_0(\kappa) = C_0(f)/(\kappa\kappa_f)^2, \tag{3.16}$$

which is less explicit in its dependence on the mapping function. However, it does allow the terms in the coefficient premultiplying χ to be examined. It can be shown that the non-negative function D_0 is such that $D_0(\kappa) = 4/45 + O(\kappa^2)$ as $\kappa \to 0$ and that $D_0(\kappa) \sim 4\kappa^{-4}$ as $\kappa \to \infty$; numerical evidence shows that D_0 is a decreasing function. Therefore, if $|\kappa'|$ is not too large the second component in the coefficient of χ in (3.12) is relatively small and χ is then approximated well by the equation

$$\chi'' + \kappa^2\chi = 0. \tag{3.17}$$

This simplification, which we will use numerical tests to examine later, is consistent with the interpretation of $||v_\xi||^2$ in (3.8) as a correction term.

3.1. *Analytic solution*

The boundary-value problem consisting of (3.12) and (3.15) can be solved numerically by truncating the domain, and we will consider this approach later. Alternatively, an analytic solution can be obtained by adapting the method given in Porter (2003). For this purpose we use the generic form

$$\chi'' + (\kappa^2 - 2\kappa e(\xi))\chi = 0, \tag{3.18}$$

which turns out to be algebraically convenient and can be applied to each of the equivalent forms (3.8), (3.12) and (3.16) by appropriate choices of e. It will be assumed that (3.14) applies so that $e(\xi)$ decays exponentially as $|\xi|$ increases.

Let $p_1(\xi)$ and $p_2(\xi)$ be defined by

$$2\mathrm{i}\kappa p_1 = \chi' + \mathrm{i}\kappa\chi, \quad -2\mathrm{i}\kappa p_2 = \chi' - \mathrm{i}\kappa\chi. \tag{3.19}$$

Since $\chi = p_1 + p_2$ and $\chi' = \mathrm{i}\kappa(p_1 - p_2)$ then

$$p_1' + p_2' = \mathrm{i}\kappa(p_1 - p_2),$$

whilst (3.18) implies that

$$\{\mathrm{i}\kappa(p_1 - p_2)\}' + (\kappa^2 - 2\kappa e)(p_1 + p_2) = 0.$$

The previous two equations can readily be rearranged as

$$p_1' = ap_1 - \bar{b}p_2, \quad p_2' = -bp_1 + \bar{a}p_2, \tag{3.20}$$

in which

$$a = \mathrm{i}\kappa + b, \quad b = -\frac{\kappa'}{2\kappa} - \mathrm{i}e.$$

The further transformations

$$q_1 = \alpha^{-1}p_1, \quad q_2 = \bar{\alpha}^{-1}p_2, \quad \alpha(\xi) = \exp\left\{\int a(\xi)\,\mathrm{d}\xi\right\}, \tag{3.21}$$

reduce (3.20) to the simple forms

$$q_1' = -\overline{m}\,q_2, \quad q_2' = -m\,q_1, \tag{3.22}$$

in which

$$m(\xi) = b(\xi)\alpha(\xi)/\overline{\alpha(\xi)}$$

is exponentially small for sufficiently large $|\xi|$ in the current applications of (3.18), as a consequence of the assumption (2.9). This construction therefore decouples the far-field components in the solution of (3.18) from the near-field effects, the latter being determined by solving (3.22).

Before completing the solution we need to define α more precisely. We take

$$\alpha(\xi) = \begin{cases} c_0\kappa^{-1/2}(\xi)\exp\left\{\mathrm{i}\kappa_0\xi + \mathrm{i}\displaystyle\int_{-\infty}^{\xi}\{\kappa(s) - \kappa_0 - e(s)\}\,\mathrm{d}s\right\}, & \xi < 0, \\[2ex] c_1\kappa^{-1/2}(\xi)\exp\left\{\mathrm{i}\kappa_1\xi - \mathrm{i}\displaystyle\int_{\xi}^{\infty}\{\kappa(s) - \kappa_1 - e(s)\}\,\mathrm{d}s\right\}, & \xi > 0, \end{cases}$$

where

$$c_0 = \exp\left\{-i \int_{-\infty}^{0} \{\kappa(s) - \kappa_0 - e(s)\}\, ds\right\}, \quad c_1 = \exp\left\{i \int_{0}^{\infty} \{\kappa(s) - \kappa_1 - e(s)\}\, ds\right\}.$$

We note that the integrands are exponentially small as $|s| \to \infty$ and that this choice ensures that $\alpha(\xi)$ is continuous for $\xi \in (-\infty, \infty)$ and such that

$$\alpha(\xi) \sim \begin{cases} c_0 \kappa_0^{-1/2} e^{i\kappa_0 \xi}, & \xi \to -\infty, \\ c_1 \kappa_1^{-1/2} e^{i\kappa_1 \xi}, & \xi \to \infty. \end{cases}$$

Applying the transformations (3.19) and (3.21) to (3.15), we find that

$$q_1 \to c_0^{-1} \kappa_0^{1/2} A_0, \quad q_2 \to \bar{c}_0^{-1} \kappa_0^{1/2} B_0 \quad \text{as } \xi \to -\infty, \tag{3.23}$$

and

$$q_1 \to c_1^{-1} \kappa_1^{1/2} B_1, \quad q_2 \to \bar{c}_1^{-1} \kappa_1^{1/2} A_1 \quad \text{as } \xi \to \infty. \tag{3.24}$$

To construct the solution of (3.22) we note that if $(X_1, X_2)^T$ satisfies the equations, that is, if

$$X_1' = -\bar{m} X_2, \quad X_2' = -m X_1, \tag{3.25}$$

then so does $(\bar{X}_2, \bar{X}_1)^T$. Therefore we can write

$$\begin{pmatrix} q_1 \\ q_2 \end{pmatrix} = E_1 \begin{pmatrix} X_1 \\ X_2 \end{pmatrix} + E_2 \begin{pmatrix} \bar{X}_2 \\ \bar{X}_1 \end{pmatrix}. \tag{3.26}$$

If we choose

$$X_1 \to 1, \quad X_2 \to 0 \quad \text{as } \xi \to -\infty, \tag{3.27}$$

then

$$E_1 = c_0^{-1} \kappa_0^{1/2} A_0, \quad E_2 = \bar{c}_0^{-1} \kappa_0^{1/2} B_0, \tag{3.28}$$

follow at once from (3.23). Further, the Wronskian W of the solutions $(X_1, X_2)^T$ and $(\bar{X}_2, \bar{X}_1)^T$ is

$$W \equiv |X_1|^2 - |X_2|^2 = 1, \tag{3.29}$$

so the pair is linearly independent and $X_1(\xi)$ is non-vanishing for $\xi \in (-\infty, \infty)$.

Applying (3.24) to (3.26) and using (3.28) we find that

$$-\begin{pmatrix} \bar{c}_0^{-1} \kappa_0^{1/2} \bar{X}_2^{\infty} & -c_1^{-1} \kappa_1^{1/2} \\ \bar{c}_0^{-1} \kappa_0^{1/2} \bar{X}_1^{\infty} & 0 \end{pmatrix} \begin{pmatrix} B_0 \\ B_1 \end{pmatrix} = \begin{pmatrix} c_0^{-1} \kappa_0^{1/2} X_1^{\infty} & 0 \\ c_0^{-1} \kappa_0^{1/2} X_2^{\infty} & -\bar{c}_1^{-1} \kappa_1^{1/2} \end{pmatrix} \begin{pmatrix} A_0 \\ A_1 \end{pmatrix}$$

and, after some simplification is carried out using (3.29), the scattering matrix defined in (2.4) takes the form

$$\mathscr{S} = \boldsymbol{\Gamma}^{-1} \mathscr{X} \bar{\boldsymbol{\Gamma}}, \tag{3.30}$$

where

$$\boldsymbol{\Gamma} = \begin{pmatrix} \bar{c}_0^{-1} \kappa_0^{1/2} & 0 \\ 0 & c_1^{-1} \kappa_1^{1/2} \end{pmatrix}, \quad \mathscr{X} = \begin{pmatrix} X_2^{\infty} (\bar{X}_1^{\infty})^{-1} & -(\bar{X}_1^{\infty})^{-1} \\ -(\bar{X}_1^{\infty})^{-1} & -\bar{X}_2^{\infty} (\bar{X}_1^{\infty})^{-1} \end{pmatrix}$$

and the notation

$$X_i^{\infty} = \lim_{\xi \to \infty} X_i(\xi)$$

has been introduced.

It remains to solve (3.25) subject to (3.27) and this is easily achieved. Integration gives

$$X_1 = g - MX_2, \quad X_2 = -UMUX_1,$$

where the operators M and U are defined by

$$(MX)(\xi) = \int_{-\infty}^{\xi} \overline{m(s)}\, X(s)\, \mathrm{d}s, \quad (UX)(\xi) = \overline{X(\xi)},$$

and $g(\xi) = 1$. It follows that X_1 satisfies the linear Volterra equation $X_1 = g + (MU)^2 X_1$ and the solution is given by the Neumann series (see, for example, Porter & Stirling 1990)

$$X_1 = \sum_{n=0}^{\infty} (MU)^{2n} g,$$

whence

$$X_2 = -U \sum_{n=0}^{\infty} (MU)^{2n+1} g.$$

We remark here that operator theory can be used to put this deduction on a secure footing and, in particular, assure convergence of these series. Computations have confirmed that the series in fact converge very rapidly, as will be clear from results given later in this section.

If we define the sequence γ_n by

$$\gamma_0(\xi) = 1, \quad \gamma_n(\xi) = (MU\gamma_{n-1})(\xi) = \int_{-\infty}^{\xi} \overline{m(s)\gamma_{n-1}(s)}\, \mathrm{d}s\, (n \in \mathbb{N}), \tag{3.31}$$

then

$$X_1(\xi) = \sum_{n=0}^{\infty} \gamma_{2n}(\xi), \quad X_2(\xi) = -\sum_{n=0}^{\infty} \overline{\gamma_{2n+1}(\xi)}. \tag{3.32}$$

Finally, we use (2.4) and (3.30) with (3.29) to give the magnitudes of the scattering coefficients in the forms

$$\left.\begin{array}{l} |R_0|^2 = |R_1|^2 = |X_2^{\infty}|^2 (1 + |X_2^{\infty}|^2)^{-1} = 1 - |X_1^{\infty}|^{-2}, \\ |T_0|^2 = (\kappa_0/\kappa_1)(1 + |X_2^{\infty}|^2)^{-1}, \quad |T_1|^2 = (\kappa_1/\kappa_0)(1 + |X_2^{\infty}|^2)^{-1}. \end{array}\right\} \tag{3.33}$$

3.2. *Numerical implementation*

In order to determine the direct numerical solution of the scattering problem from (3.12) it is convenient to express the equation as the first-order system

$$\begin{pmatrix} \chi(\xi) \\ \chi'(\xi) \end{pmatrix}' = \begin{pmatrix} 0 & 1 \\ -(\kappa^2 - C_0(f)f'^2) & 0 \end{pmatrix} \begin{pmatrix} \chi(\xi) \\ \chi'(\xi) \end{pmatrix}. \tag{3.34}$$

From the assumed far-field forms of $\chi(\xi)$ as $\xi \to \pm\infty$ given by (3.15), which are assumed to hold exactly for $\xi \leqslant a$ and $\xi \geqslant b$ we can easily determine the relations

$$\left.\begin{array}{l} \boldsymbol{P}^T \boldsymbol{\chi}(a) = 2\mathrm{i}\kappa_0 A_0 \mathrm{e}^{\mathrm{i}\kappa_0 a}, \\ \overline{\boldsymbol{P}}^T \boldsymbol{\chi}(a) = -2\mathrm{i}\kappa_0 B_0 \mathrm{e}^{-\mathrm{i}\kappa_0 a} \end{array}\right\} \tag{3.35}$$

and

$$\left.\begin{array}{l} \boldsymbol{Q}^T \boldsymbol{\chi}(b) = 2\mathrm{i}\kappa_1 A_1 \mathrm{e}^{-\mathrm{i}\kappa_1 b}, \\ \overline{\boldsymbol{Q}}^T \boldsymbol{\chi}(b) = -2\mathrm{i}\kappa_1 B_1 \mathrm{e}^{\mathrm{i}\kappa_1 b}, \end{array}\right\} \tag{3.36}$$

where $\boldsymbol{P}^T = (\mathrm{i}\kappa_0, 1)$, $\boldsymbol{Q}^T = (\mathrm{i}\kappa_1, -1)$ and $\boldsymbol{\chi}^T(\xi) = (\chi(\xi), \chi'(\xi))$. The parameters a and b are established numerically by an iterative process in which a and b assume a sequence of increasingly negative and positive values until quantities of interest have converged to within a required tolerance. This process is very quick (typically one or two iterations) since, outside some interval, the dependence of the solution on x is exponentially small – see (3.14).

Now the general solution of (3.34) can be written as

$$\boldsymbol{\chi}(\xi) = \boldsymbol{\Psi}(\xi)\boldsymbol{E},$$

where $\boldsymbol{E}$ is an arbitrary constant vector and $\boldsymbol{\Psi}(\xi)$ is a 2×2 matrix, the columns of which are linearly independent solutions of the equation. Using this expression in (3.35) and (3.36) to eliminate $\boldsymbol{E}$, we recover the scattering matrix formulation given in (2.4) with

$$\mathscr{S} = -\mathscr{D}\mathscr{K}^{-1} \begin{pmatrix} \overline{\boldsymbol{P}}^T \boldsymbol{\Psi}(a) \\ \overline{\boldsymbol{Q}}^T \boldsymbol{\Psi}(b) \end{pmatrix} \begin{pmatrix} \boldsymbol{P}^T \boldsymbol{\Psi}(a) \\ \boldsymbol{Q}^T \boldsymbol{\Psi}(b) \end{pmatrix}^{-1} \mathscr{K}\mathscr{D}$$

where

$$\mathscr{D} = \begin{pmatrix} \mathrm{e}^{\mathrm{i}\kappa_0 a} & 0 \\ 0 & \mathrm{e}^{-\mathrm{i}\kappa_1 b} \end{pmatrix}, \qquad \mathscr{K} = \begin{pmatrix} \kappa_0 & 0 \\ 0 & \kappa_1 \end{pmatrix}.$$

The relationship (2.5) can easily be seen to be satisfied, whatever $\boldsymbol{\Psi}(a)$ and $\boldsymbol{\Psi}(b)$.

The scattering matrix is thus determined by the value of $\boldsymbol{\Psi}(b)$ as a function of the prescribed matrix $\boldsymbol{\Psi}(a)$, the most obvious choice for the latter being the 2×2 identity matrix. Thus the columns of the matrix $\boldsymbol{\Psi}(b)$ are obtained by solving two initial-value problems for (3.34) over the range $a \leqslant \xi \leqslant b$, one with $\chi(a) = 1$, $\chi'(a) = 0$ and the second with $\chi(a) = 0$, $\chi'(a) = 1$. A standard numerical integration solver can be used for this purpose.

A second method of determining the solution of the scattering problem uses the analytic solution derived in §3.1. The aim is not to provide a computational approach that is comparable to the direct numerical solution but to determine the accuracy of the simple explicit approximations that are given by small values of N. There are two sources of error in calculating the exact expressions for the reflection and transmission coefficients by means of (3.33). The first is in the numerical approximation of the improper integrals defining $\alpha(\xi)$ and the sequence $\gamma_n(\xi)$. In our results, the aim has been to calculate these integrals to five-decimal-place accuracy. The second source of error is in the truncation of the infinite series defining X_1^∞ and X_2^∞ in (3.32). When $\gamma_n(\xi)$ has been calculated recursively from (3.31) for $n = 1, \dots, N$ then N will be referred to as the truncation parameter. Consequently, if N is even, $|R_0|$ will be defined in terms of X_1^∞ and if N is odd, X_2^∞ will be used to define $|R_0|$. Hence, the lowest-order approximation will be for $N = 1$ when $X_2^\infty = -\lim_{\xi \to \infty} \overline{\gamma_1(\xi)}$ and then for $N = 2$, $X_1^\infty = \lim_{\xi \to \infty} \gamma_2(\xi)$ and so on.

3.3. *Examples*

Mapping functions

We shall concentrate on three different families of bed profile including some special cases of the mappings considered by Fitz-Gerald (1976).

The first bed shape we consider is generated by the transformation

$$h_0^{-1} F(\zeta) = \zeta + (\pi\beta)^{-1}(\epsilon - 1)\ln(1 + \mathrm{e}^{\beta\pi\zeta}),$$
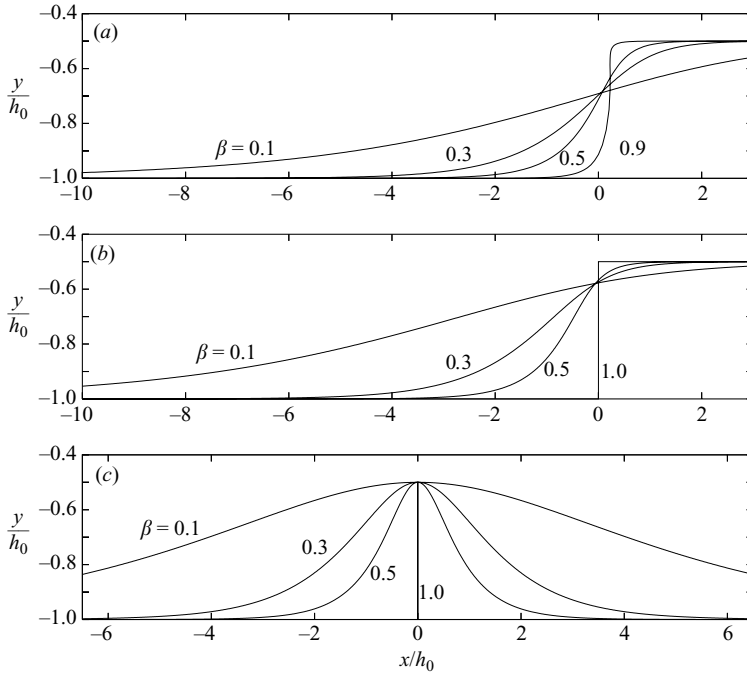
FIGURE 1. A selection of bed profiles for each of the three mappings with varying values of β (shown against curves): (a) the Roseau profile, (b) the shoaling profile, $\alpha = \frac{1}{2}\pi$ and (c) the ridge profile. In each case the depth ratio $\epsilon = \frac{1}{2}$.

where the parameter $\beta \in (0, 1)$ and the far-field depth ratio $\epsilon = h_1/h_0$ is assumed to satisfy $\epsilon \in (0, 1)$. The corresponding free-surface variation is

$$f(\xi) = K h_0 (1 + \epsilon e^{\beta\pi\xi})/(1 + e^{\beta\pi\xi}). \tag{3.37}$$

This mapping was originally used by Roseau (1976) who exploited its particular form to determine what is still the only known explicit and exact expression for the modulus of the reflection coefficient for the unapproximated linearized water wave equations over a variable bed, which (in the current notation) is given by

$$|R_0| = |R_1| = \left| \frac{\sinh(\kappa_0 - \kappa_1)/\beta}{\sinh(\kappa_0 + \kappa_1)/\beta} \right|. \tag{3.38}$$

The bed profile consists of a smooth monotonic transition from the depth h_0 to the depth $h_1 < h_0$, the parameter β controlling the width of the transition. As $\beta \to 0$ the transition width increases indefinitely and as $\beta \to 1$ the bed steepens and eventually forms an overhang (see $\beta = 0.9$ in figure 1a).

It is worth briefly remarking upon the limiting value of $\beta = 1$, since this appears to have been overlooked in previous work on the Roseau profile. The mapping for $\beta = 1$ is a highly singular limit of the family of mappings since it represents a semi-infinite horizontal plate of zero thickness submerged to a depth h_1, detached from an infinite horizontal bed of depth h_0. Clearly, with $\beta = 1$ (3.37) is still well-defined and a solution can be found to the problem in the ζ-plane. This solution, however, corresponds to an unphysical scattering problem in the z-plane, since the mapping

of the point $\zeta = -\mathrm{i}$ to infinity under the plate in the z-plane implies an unprescribed source of mass flux under the plate.

The second of the mappings we consider also represents a family of shoaling bed profiles from the depth h_0 to the depth $h_1 < h_0$ over a transition width determined again by a parameter β, where now $\beta \in (0, 1]$. For $\beta = 1$, the change from the depth h_0 to h_1 occurs by means of a plane slope making an angle α to the positive x-axis. This linear bed profile is often named after Booij (1983), who used it to assess the accuracy of the mild-slope equation of Berkhoff (1976) and Smith & Sprinks (1975). In this case

$$f(\xi) = K h_0 \frac{\left(1 + \epsilon^{\pi/\alpha} \mathrm{e}^{\beta\pi\xi}\right)^{\alpha/\pi}}{\left(1 + \mathrm{e}^{\beta\pi\xi}\right)^{\alpha/\pi}}. \tag{3.39}$$

For the particular value $\alpha = \frac{1}{2}\pi$ (with $\beta = 1$), the transition from the depth h_0 to h_1 occurs by means of a vertical step (see Fitz-Gerald 1976, with $\gamma = 1$ in his mapping, and Evans & Linton 1994) and for $\alpha \in (\frac{1}{2}\pi, \pi)$ there is an overhanging bed profile. For $\beta < 1$ we recover the surface variation function (3.37) of the Roseau (1976) mapping as $\alpha \to \pi$ and for each $\alpha \leqslant \pi$ decreasing values of β result in a smooth profile of increasing width which tends to infinity as $\beta \to 0$.

In general the mapping corresponding to (3.39) above cannot be determined explicitly. However, if $\alpha = \frac{1}{2}\pi$ (as considered by Fitz-Gerald 1976) we find that

$$h_0^{-1} F(\zeta) = \frac{2\epsilon}{\pi\beta} \ln \left[\frac{\epsilon w_2(\zeta) + w_1(\zeta)}{(1 - \epsilon^2)^{1/2}} \right] - \frac{1}{\pi\beta} \ln \left[\frac{w_2(\zeta) + w_1(\zeta)}{w_2(\zeta) - w_1(\zeta)} \right],$$

in which

$$w_1(\zeta) = (1 + \epsilon^2 \mathrm{e}^{\beta\pi\zeta})^{1/2}, \quad w_2(\zeta) = (1 + \mathrm{e}^{\beta\pi\zeta})^{1/2}.$$

Finally, a family of bed elevations in the form of symmetric ridges with $h_1 = h_0$ which protrude to a maximum height a above h_0, are also considered by Fitz-Gerald (1976) (by taking $l = L_0 = 0$ in his paper). Here, the relevant mapping function is given by

$$h_0^{-1} F(\zeta) = \zeta + \frac{1}{\pi\beta} \ln \left[\frac{1 - \sin^2 \rho \tanh\left(\frac{1}{2}\pi\beta\zeta\right) + \cos \rho \left(1 - \sin^2 \rho \tanh^2\left(\frac{1}{2}\pi\beta\zeta\right)\right)^{1/2}}{1 + \sin^2 \rho \tanh\left(\frac{1}{2}\pi\beta\zeta\right) + \cos \rho \left(1 - \sin^2 \rho \tanh^2\left(\frac{1}{2}\pi\beta\zeta\right)\right)^{1/2}} \right], \tag{3.40}$$

where $\cos \rho = \sin(\frac{1}{2}\pi\beta\epsilon)/\sin(\frac{1}{2}\pi\beta)$, with $\epsilon = 1 - a/h_0$ as before representing the ratio of minimum to maximum fluid depths, and this leads to

$$f(\xi) = K h_0 \cos \rho \left(1 - \sin^2 \rho \tanh^2 \left(\tfrac{1}{2}\beta\pi\xi\right)\right)^{-1/2}$$

(note the typographical error in Evans & Linton 1994 in the power of the final term). Here $\beta \in (0, 1]$ again represents the transition width of the topography. Letting $\beta \to 1$ reduces the elevation to a thin vertical barrier of length a and as $\beta \to 0$, the bed gradient tends to zero as the width of the ridge tends to infinity.

The actual curve defining the bed is given parametrically from the mapping function $F(\zeta)$ by

$$x(\xi) + \mathrm{i}y(\xi) = F(\xi - \mathrm{i}), \quad -\infty < \xi < \infty. \tag{3.41}$$

When $F(\zeta)$ cannot be found explicitly (as in the case of a shoaling bed of general angle α, for example) but the function $f(\xi)$ is known and tends to $K h_0$ as $\xi \to -\infty$,
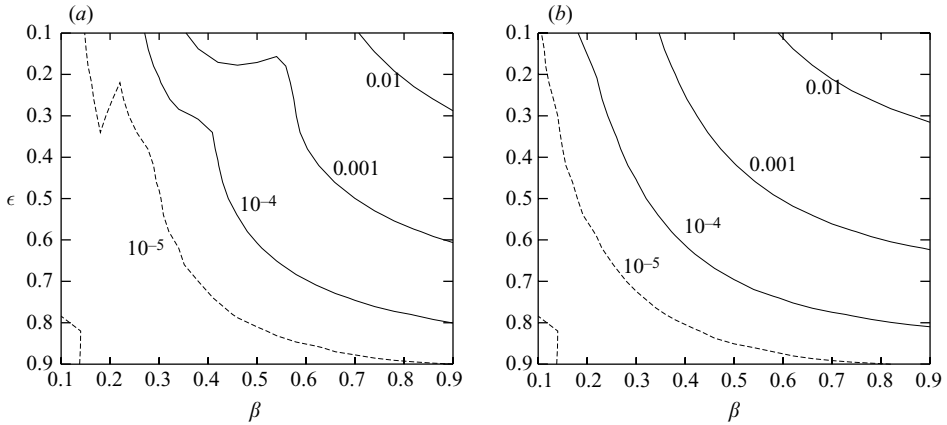
FIGURE 2. Boundaries of the error, (a) $\max_{Kh_0}\{||R_0| - |R_0|_{exact}|\}$ and
(b) $\max_{Kh_0}\{||R_0|_{approx} - |R_0|_{exact}|\}$, for the Roseau profile in (β, ϵ) parameter space.

the formula

$$\frac{z}{h_0} = \frac{x(\xi)}{h_0} + \mathrm{i}\frac{y(\xi)}{h_0} = \xi + \int_{-\infty}^{\xi} \left\{(Kh_0)^{-1} f(\xi') - 1\right\} \mathrm{d}\xi' - \mathrm{i}\int_0^1 (Kh_0)^{-1} f(\xi - \mathrm{i}\eta')\, \mathrm{d}\eta', \quad (3.42)$$

in which the integrals can be approximated numerically, can be used to determine the bed profile.

We remark that the mapping function $F(\zeta)$ is not needed to determine either the reflection and transmission coefficients or the bed profile. Since only $\mathrm{d}z/\mathrm{d}\zeta = F'(\zeta)$ is required, the task of developing new mappings is not as difficult as it might first appear.

The three different types of bed profile are illustrated in figure 1 for various values of β, having been computed using (3.41).

Error assessment for the Roseau profile

We can use the explicit result (3.38) of Roseau (1976) to perform a rigorous investigation of the accuracy of the present method over a range of parameter values. This will also enable us to assess the relative merits of the approximate versions of the method. Thus, we shall regard the numerical solution of the full differential equation (3.12) as being the unapproximated version. The reduced equation (3.17) provides us with a substantially simplified version of (3.12) and its success relies upon $C_0(f)f'^2$ being small in comparison with κ^2, which is certainly to be expected if the original bedform is slowly varying.

In figure 2(a) we illustrate the error (maximized over Kh_0) between the values of $|R_0|$ computed from the unapproximated equation with the exact results of Roseau given by (3.38). This is achieved by sketching contours of the surface generated by the error in (β, ϵ) parameter space. These marked contours act as dividing lines between regions of error. In figure 2(b), a similar plot is given for the reduced version of the equation, (3.17). Clearly the method performs very well over almost the entire range of parameters, with accuracy only dropping below 0.01 when both ϵ is small and β is close to one. In such situations, there is a large ratio between the depths at infinity (and incidentally the maximum value of $|R_0|$ is large) whilst the bed profile throughout the whole region where the error is greater than 0.01 contains an
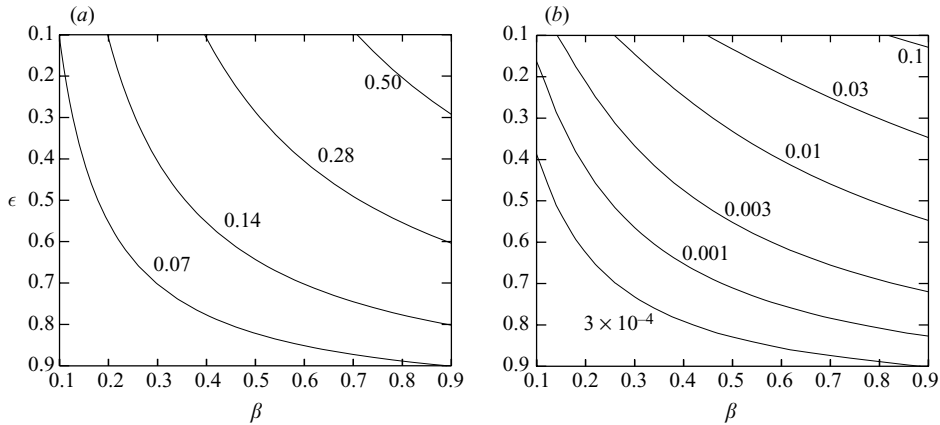
FIGURE 3. Boundaries of (a) $\max_\xi\{|f'(\xi)|/Kh_0\}$ and (b) $\max_{\{Kh_0,\xi\}}\{C_0(f)f'^2/\kappa^2\}$ for the Roseau profile in (β, ϵ) parameter space.

overhang. For moderate to small steepness in the bed profiles the present method works exceptionally well.

As remarked previously, the success of the method is due to the way in which the transformation $z = F(\zeta)$ maps large bed gradients into much smaller gradients in the function $f(\xi)$. Thus, in figure 3 we show certain dividing lines in the values of $M = \max_\xi\{|f'(\xi)|/Kh_0\}$ for the Roseau profile across the same range of parameters as in figure 2. There is a clear correspondence between the error in the values of $|R_0|$ and the value of M. Comparison with other exact results presented later on confirms the link between the value of M and the error, both qualitatively and quantitatively. Thus, if $M < 0.5$ one can expect results to within 0.01 of the true result, and an extra decimal place in accuracy is gained when $M < 0.28$ and so on.

In figure 3(b) we show dividing lines in the value of the quantity $C_0(f)f'^2/\kappa^2$, maximised over all ξ and Kh_0 in (β, ϵ) space. The reduced version of the differential equation neglects the contribution of this term on the basis that its value is much less than unity. It can be seen that it does indeed only make a relatively small contribution across all values of β and ϵ, which is at its largest when f'/Kh_0 is largest. It is of no suprise that the reduced equation is more successful at imitating the results of the unapproximated version when these values decrease towards zero.

We next compare, in figure 4(a, b), results for the reflected amplitudes obtained using the analytic solution of §3.1 with the exact values of Roseau, the aim here being to determine the effect of the truncation of the infinite series defining $|R_0|$ upon their accuracy. If the terms in the series have been calculated exactly, these expressions for $|R_0|$ are expected to converge to the solution of the full equation as more terms are included in the series. A one-term approximation (i.e. $N = 1$) is shown in figure 4(a) by the solid lines, and the dashed lines are the corresponding calculation with $e(\xi) = 0$. With $N = 3$ it can be seen in figure 4(b), with reference to figure 2(a), that the results have essentially converged to the direct numerical solution of the corresponding equation. Numerical errors due to a rather crude numerical computation of certain improper integrals affect the results when both the error is small and also when β is small and consequently the bed transition width is large. We have omitted results with $N = 2$, which, according to the convention outlined in §3.2, corresponds to defining $|R_0|$ in terms of X_1^∞ and produces far greater error than for $N = 1$ which defines $|R_0|$ in terms of $X_2^\infty = -\overline{\gamma_1}(\infty)$.
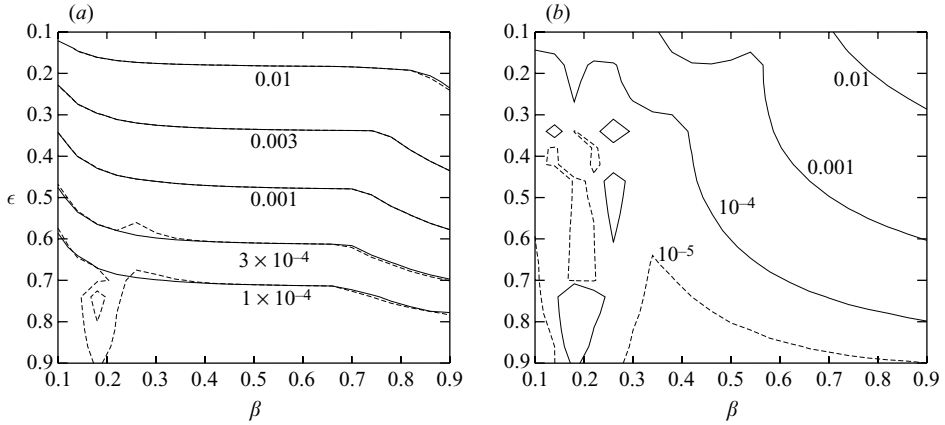
FIGURE 4. Boundaries of $\max_{Kh_0}\{||R_0|_N - |R_0|_{exact}|\}$, the difference in reflected amplitudes between the exact solution and the truncated series with (a) $N = 1$ (overlaid dashed lines corresponding to taking $e(\xi)=0$) and (b) $N = 3$ terms in (β, ϵ) parameter space.

It would therefore appear that truncation to a single term produces fairly good approximations to the reflection coefficients, which are more sensitive to the shoaling ratio than the steepness of the bed. See figure 4(a), where, for example, we observe that provided the shoaling ratio is less than 2:1, we expect a maximum error over all frequencies of less than 0.002 in $|R_0|$ even when the bed slope becomes vertical in places ($\epsilon = 0.5$, $\beta = 0.9$ is shown in figure 1). Furthermore, the simplification that arises from neglecting the $e(\xi)$ term (which corresponds to using the reduced differential equation) appears to have little effect on the results. A version of the single-term approximation is given in the conclusions.

We remark that, if (3.37) is used in the condition $|f'| \ll \kappa f$ that f be slowly varying, general qualitative deductions can be made relating the accuracy of the approximation to β and ϵ. These deductions are consistent with, but inevitably less precise and useful than, the error estimates that we have derived by comparing exact and approximate solutions.

Other results

In figure 5(a, b) $|R_0|$ is plotted against Kh_0 for the shoaling bed profile given by the free-surface variation in (3.39) with $\alpha = \frac{1}{2}\pi$, for a range of values of β and two shoaling ratios of $\epsilon = h_1/h_0 = 0.5$ and 0.1. In each case results for $\beta = 1$, corresponding to a vertical step in the bed, are compared with those of Porter (1995) who was able to obtain accuracy to five decimal places using an integral equation formulation of the problem which exploited the rectangular geometry. In this most extreme case, $M = \max_\xi\{f'(\xi)/Kh_0\} = 0.38$ for $\epsilon = 0.5$ and $M = 0.6$ for $\epsilon = 0.1$. With reference to the earlier discussion it is not surprising that the agreement between the 'exact' results and those obtained from this method are not so good, but acceptable estimates are nevertheless obtained. The other curves in figure 5(a, b) are for a decreasing sequence of values of $\beta \leqslant 0.7$. The values of M for $\epsilon = 0.1$ and $\epsilon = 0.5$ decrease as β is reduced and are $M = 0.26$ and $M = 0.41$ (respectively) for $\beta = 0.7$, the implication being that those results are in much closer agreement than those for $\beta = 1$.

The reflected wave amplitude corresponding to the special case of the plane slope, for which $f(\xi)$ is given by (3.39) with $\beta = 1$, is displayed in figure 6. The 'exact' solution for this bed profile was derived by Booij (1983) using a numerical method
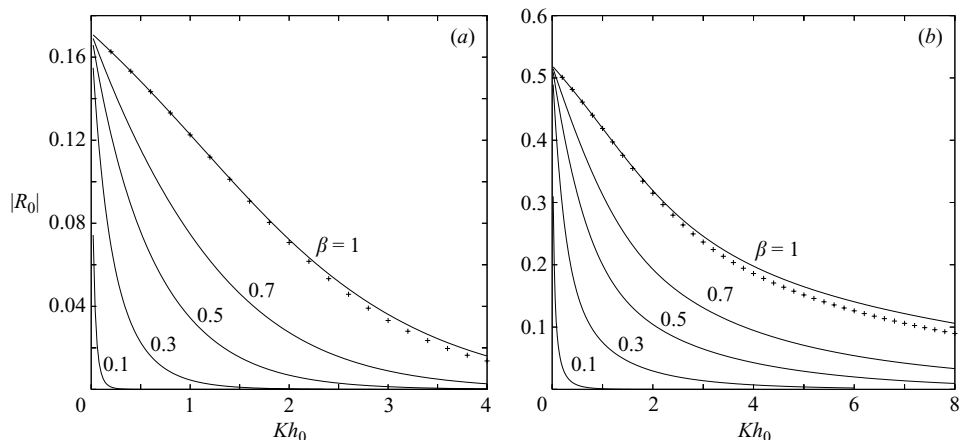
FIGURE 5. Reflection coefficient for shoaling bed profile with $\alpha = \frac{1}{2}\pi$ given by the mapping (3.39) and different values of β (shown against curves): (a) $h_1/h_0 = 0.5$; (b) $h_1/h_0 = 0.1$. The crosses represent 'exact' results for the vertical step.
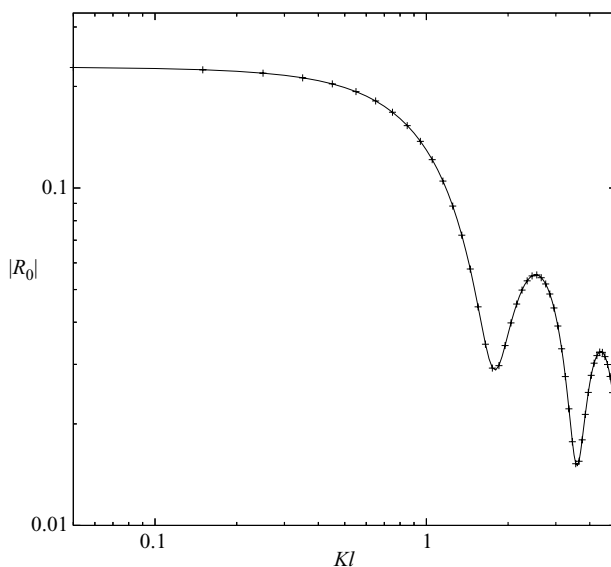

FIGURE 6. Reflection coefficient for the Booij bed profile: $h_1/h_0 = \frac{1}{3}$, $Kh_0 = 0.6$, length of sloping bed is l. The crosses represent 'exact' results from full linear theory.

for the parameter values $h_1/h_0 = \frac{1}{3}$, $Kh_0 = 0.6$, l denoting the length of sloping bed, and it has become a standard test problem against which to measure the accuracy of approximation techniques. However, the 'exact' solution used in figure 6 is provided by the integral equation method of Porter & Porter (2000). The high accuracy of the present approximation, although impressive, is in part due to the fact that the Booij profile is incapable of assessing the effects of non-zero bed curvature on approximations and these can be significant. The mapping function is not given explicitly in this case but, as we remarked earlier, only its slope is required to approximate the scattering properties. Bender & Dean (2003) have recently considered
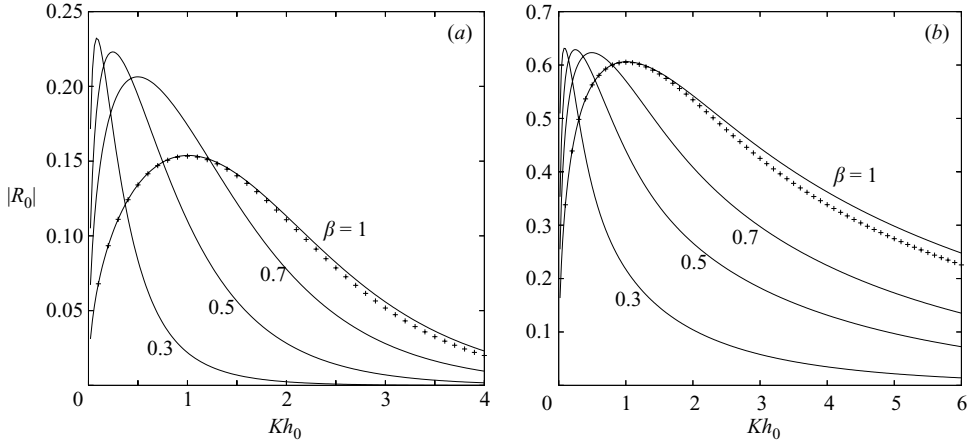
FIGURE 7. Reflection coefficient for symmetric bed profiles given by the mapping (3.40) with different values of β (shown against curves): (a) $a/h_0 = 0.5$; (b) $a/h_0 = 0.9$. The crosses represent 'exact' results for the vertical barrier.

$(Kh_0, \beta, a/h_0)$	$(1, 1, 0.5)$	$(0.1, 1, 0.5)$	$(1, 1, 0.9)$
ODE (full)	0.1537	0.0680	0.6061
ODE (reduced)	0.1530	0.0679	0.6045
Step approx.	0.1529	0.0679	0.6042
Exact	0.1533	0.0680	0.6054

TABLE 1. Comparison between 'exact' results of Porter & Evans (1995) for $|R_0|$ in the case of scattering by a thin vertical barrier, and the solution to the full equation (3.12) and the reduced version (3.17). Also shown are the results of Evans & Linton's (1994) 'step approximation' method with $N = 100$ discretizations.

scattering by a number of piecewise-linear bedforms, including a trench with sloping sides, to which the present method may readily be applied by using the slope of the corresponding Schwarz–Christoffel mapping function.

Results for the mapping function (3.40) that describes a symmetric ridge are given in figure 7. We have also included, in table 1, for the limiting case $\beta = 1$ of a thin vertical barrier a comparison between the 'exact' results (accurate to the number of decimal places quoted) of Porter & Evans (1995) based on integral equation techniques and the present method (including the reduced version of the differential equation) at three sets of parameter values chosen to allow Evans & Linton's (1994) step approximation with $N = 100$ discretizations, described earlier, to be included. The present method produces extremely accurate results for the frequency range $0 < Kh_0 \leqslant 1$ covered in the table but for higher frequencies it does not perform so well, as illustrated in figure 7. There, with $\beta = 1$, the maximum values of $M = |f'|/(Kh_0)$ are 0.3 and 0.6 for $h_1/h_0 = 0.5$ and 0.1 (respectively). In the former example, the relatively poor quality of the results obtained by solving the differential equation may be explained by the large value of $|f''|$, not experienced in the previous mappings considered. This substantiates the earlier comment on the shortcomings of the Booij bedform as a reliable test case.

4. More general topography

The obvious drawback in the method described so far is that it is restricted to topography for which there is a conformal mapping. We now suppose therefore that the given depth function can be written as $h(x) = h^{(0)}(x) - h^{(1)}(x)$, where $h^{(0)}$ corresponds to a known mapping (which we continue to denote by $z = F(\zeta)$ for convenience) such that $y = -h^{(0)}(x)$ maps onto $\eta = -1$, and $h^{(1)} > 0$ represents a slowly varying component of the topography. It is assumed that $h^{(1)}(x) \to 0$ as $|x| \to \infty$, which ensures that (2.1) holds. The whole bedform $y = -h(x)$ maps onto $\eta = -d(\xi) \geqslant -1$, say, where $d(\xi) \to 1$ as $|\xi| \to \infty$ and $d(\xi)$ is slowly varying.

We therefore envisage a more general topography than hitherto in which the steep component is taken account of by the conformal mapping and slow variations about this component remain in the boundary condition on the transformed bed. This structure is confirmed by the transformed boundary value problem

$$\left. \begin{aligned} \varphi_{\xi\xi} + \varphi_{\eta\eta} &= 0, \quad -\infty < \xi < \infty, -d(\xi) < \eta < 0, \\ \varphi_\eta + d'(\xi)\varphi_\xi &= 0, \quad -\infty < \xi < \infty, \ \eta = -d(\xi), \\ \varphi_\eta - f(\xi)\varphi &= 0, \quad -\infty < \xi < \infty, \eta = 0. \end{aligned} \right\} \tag{4.1}$$

Here $f(\xi) = KF'(\xi)$ as before and our assumptions imply that (2.7) and (2.8) remain in force. The problem therefore generalizes (2.2) and (2.6) and includes both as special cases.

A modification of our previous method is used to approximate the solution of (4.1) and we give the essential steps, using the same notation as before to represent the corresponding quantities. The functional L defined in (3.1) is modified to

$$L(\psi) = \frac{1}{2} \int_a^b \left\{ \int_{-d(\xi)}^0 (\psi_\xi^2 + \psi_\eta^2) \, \mathrm{d}\eta - f(\xi)(\psi^2)_{\eta=0} \right\} \mathrm{d}\xi,$$

and its first variation is

$$\delta L = \int_a^b \left\{ ((\psi_\eta - f(\xi)\psi)\delta\psi)_{\eta=0} - ((\psi_\eta + d'(\xi)\psi_\xi)\delta\psi)_{\eta=-d(\xi)} \right.$$
$$\left. - \int_{-d(\xi)}^0 (\psi_{\xi\xi} + \psi_{\eta\eta})\delta\psi \, \mathrm{d}\eta \right\} \mathrm{d}\xi + \left[\int_{-d(\xi)}^0 \psi_\xi \delta\psi \, \mathrm{d}\eta \right]_{\xi=a}^{\xi=b}. \tag{4.2}$$

Therefore L is stationary at the solution of (4.1), assuming that $\delta\psi = 0$ at $\xi = a, b$ as usual.

The approximation corresponding to (3.6) is

$$\varphi(\xi, \eta) \approx \psi(\xi, \eta) = \chi(\xi)v(\xi, \eta), \quad v(\xi, \eta) = s(\kappa(\xi), d(\xi))\cosh\kappa(\xi)(\eta + d(\xi)) \tag{4.3}$$

in which $\kappa(\xi)$ is now the positive real root of

$$f(\xi) = \kappa(\xi)\tanh(\kappa(\xi)d(\xi)). \tag{4.4}$$

This parallels the earlier approximation, the η dependence in ψ being the eigenfunction v that corresponds to propagating waves with f and d constant, at each local value of f and each local depth d. The normalizing factor s in v will be chosen later.

Using (4.2) we readily find that the effect of applying the variational principle $\delta L = 0$ to the approximation (4.3), with $\delta\chi = 0$ at $\xi = a, b$, is the equation

$$\int_{-d(\xi)}^0 ((\chi v)_{\xi\xi} + (\chi v)_{\eta\eta}) v \, \mathrm{d}\eta + d'(\xi)((\chi v)_\xi v)_{\eta=-d(\xi)} = 0.$$

This can be rearranged in the form

$$(||v||^2\chi')' + \{\kappa^2||v||^2 + (v, v_\xi)_\xi - ||v_\xi||^2\}\chi = 0, \tag{4.5}$$

in which the revised inner product is defined by

$$(u, v) = \int_{-d(\xi)}^0 u\bar{v}.$$

The local dispersion relation (4.4) can be regarded as defining the function $\kappa = \kappa(f, d)$ with first derivatives

$$\kappa_d = -2\kappa^2(2\kappa d + \sinh 2\kappa d)^{-1}, \quad \kappa_f = (1 + \cosh 2\kappa d)(2\kappa d + \sinh 2\kappa d)^{-1}. \tag{4.6}$$

Thus

$$v_\xi = v_d d' + v_f f',$$

and similarly for $(v, v_\xi)_\xi$, leading to the version

$$(||v||^2\chi')' + \{\kappa^2||v||^2 + (v, v_d)d'' + (v, v_f)f'' + ((v, v_d)_d - ||v_d||^2)d'^2$$
$$+ ((v, v_d)_f + (v, v_f)_d - 2(v_d, v_f))d'f' + ((v, v_f)_f - ||v_f||^2)f'^2\}\chi = 0 \tag{4.7}$$

of (4.5).

We note on setting $d = 1$ in (4.7) that the equation (3.12) derived earlier owes its relative simplicity to the normalization $||v|| = 1$, which implies that $(v, v_f) = 0$, and (3.12) then follows using (3.9). This is the only choice of scaling that removes the term involving f'' and leads to the simplified version (3.17) of (3.9). On the other hand if we let $f = $ constant, (4.7) reduces to the modified mild-slope equation

$$(||v||^2\chi')' + \{\kappa^2||v||^2 + (v, v_d)d'' + ((v, v_d)_d - ||v_d||^2)d'^2\}\chi = 0,$$

which approximates the solution of the boundary value problem (2.2) when the original notation is restored. The standard form derived by Chamberlain & Porter (1995) corresponds to the choice $s = \mathrm{sech}\,\kappa d$ in (4.3), which follows Berkhoff (1976) and subsequent authors, and has the advantage that $\psi(\xi, 0) = \chi(\xi)$ is proportional to the free-surface elevation. The alternative scaling in which s is such that $||v|| = \kappa^{-1}$ leads to the simplified version of the modified mild-slope equation,

$$(\kappa^{-2}\chi')' + \{1 - U_0(d)d'^2\}\chi = 0,$$
$$U_0(d) = ||u||^{-4}k^{-2}\{||u||^2||u_d||^2 - (u, u_d)^2\}, \quad u = u(d, \eta) = \cosh\kappa(\eta + d),$$

which was derived in Porter (2003) and parallels (3.12).

We can therefore simplify (4.7) when either d or f is constant, by different choices of the normalizing factor s. It is perhaps worth drawing attention here to the essential difference between these two special cases, which is that the integral defining the inner product involves $d(\xi)$ in the lower limit.

In the general case that we are interested in here, we take $||v|| = 1$ in order to preserve the form of the earlier equation (3.12) and, in particular, the applicability of the earlier analytic solution. To implement this normalization, we write

$$v = ||w||^{-1}w, \quad w = w(f, d, \eta) = \cosh\kappa(\eta + d).$$

A straightforward calculation then shows that (4.7) can be expressed in the form

$$\chi'' + \{\kappa^2 - \tfrac{1}{2}||w||^{-2}d'' - C_0 f'^2 - C_1 d'^2 - C_2 f'd'\}\chi = 0, \tag{4.8}$$

which is the extension of (3.12). Here, C_0 is given by (3.13), although it now depends on f and d because of the change in w, and

$$C_1 = ||w||^{-4}\{||w||^2||w_d||^2 - ((w, w_d) + \tfrac{1}{2})^2\},$$
$$C_2 = ||w||^{-4}\{2||w||^2(w_f, w_d) - (w, w_f) - 2(w, w_f)(w, w_d)\}.$$

Evaluating the inner products arising here, we find that

$$4\kappa||w||^2 = r + \sinh r, \quad 8\kappa^2(w, w_f) = (r\cosh r - \sinh r)\kappa_f,$$
$$8\kappa^2(w, w_d) = (r\cosh r - \sinh r)\kappa_d + 2(\cosh r - 1)\kappa^2, \quad 8\kappa^3||w_f||^2 = A\kappa_f^2,$$
$$8\kappa^3(w_f, w_d) = A\kappa_f\kappa_d + B\kappa^2\kappa_f, \quad 8\kappa^3||w_d||^2 = A\kappa_d^2 + B\kappa^2\kappa_d + 4(\sinh r - r)\kappa^2,$$

where

$$6A = 3r^2\sinh r - 6r\cosh r + 6\sinh r - r^3, \quad 2B = 2r\sinh r - 2\cosh r + 2 - r^2,$$

$r = 2\kappa d$ and κ_f and κ_d are given by (4.6).

We note that (4.8) applies only where d' is continuous and that the jump condition

$$2||w||^2[\chi'] = [d']\chi,$$

which easily follows from the differential equation, applies across locations where it is not continuous. The notation [ ] denotes the jump in the included quantity. This means that the approximation $\psi \approx \varphi$ is such that ψ_ξ is discontinuous where d' is, a feature of the standard mild-slope equation (see Porter 2003, for example).

4.1. *An example*

We provide just one set of results illustrating the application of the theory developed in this section. We concentrate on the Booij profile involving a plane slope of angle $\alpha = \tfrac{1}{4}\pi$ connecting the level depths $h_0 < h_1 = \tfrac{1}{3}h_0$. Thus the free-surface variation is defined by (3.39) with $\alpha = \tfrac{1}{4}\pi$ and $\beta = 1$. In the mapped ζ-plane we replace the horizontal bottom of the fluid, $\eta = -1$, by the variable bed profile $\eta = -d(\xi)$, where

$$d(\xi) = \begin{cases} 1 - \tfrac{1}{20}(1 + \cos(\pi(\xi - c))), & |\xi - c| \leqslant 1, \\ 1, & |\xi - c| > 1, \end{cases}$$

which represents a symmetric protrusion in the interval $c - 1 < \xi < c + 1$ rising with continuous gradient from the level $\eta = -1$ whose maximum height is just one tenth of the width of the strip (in the ζ-plane). This small-amplitude perturbation certainly conforms with theory developed above.

In this case, and more generally, the bed shape in the physical plane is then implicitly given by

$$x(\xi)/h_0 + \mathrm{i}y(\xi)/h_0 = F(\xi - \mathrm{i}d(\xi)).$$

When the mapping function $F(\zeta)$ is not known, (3.42) can be used with the upper limit on the second integral replaced by $d(\xi)$. The physical bed shape is therefore given by an inverse procedure, although it is possible to derive an effective algorithm for determining the function $d(\xi)$ from a given $h(x)$.

Returning to the specific example considered here, the value of c is given the discrete values 0, $\tfrac{1}{2}$, 1 and $\tfrac{3}{2}$, which has the effect in the ζ-plane of shifting the cosine-shaped protrusion along the ξ-axis. The resulting bed profiles in the physical plane are illustrated in figure 8(*a*). Curves showing the variation of $|R_0|$ with wavenumber resulting from each value of c is shown in figure 8(*b*). For example, when $c = 0$, there is a significant modification of the bed which smoothes the otherwise sharp join at the
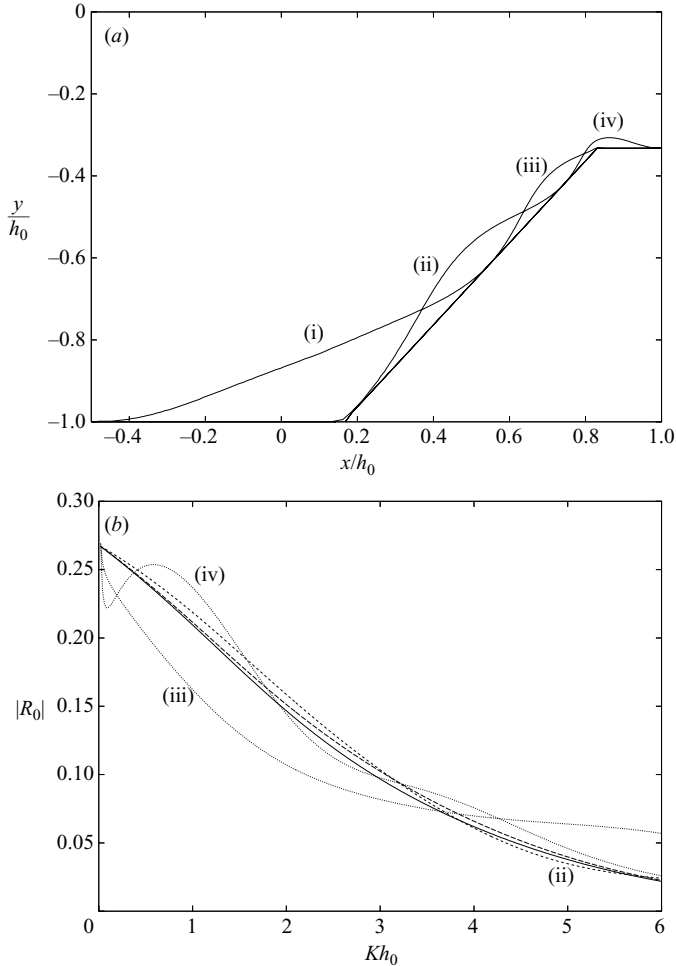
FIGURE 8. Reflection coefficient for sloping bed profiles given by the mapping function (3.38) with $\alpha = \frac{1}{4}\pi$, $\beta = 1$, $\epsilon = \frac{1}{3}$ upon which a cosine profile $d(\xi) = 1 - \frac{1}{20}(1 + \cos(\pi(\xi - c)))$, $|\xi - c| < 1$ is superimposed with (i) $c = 0$ (long dashed); (ii) $c = \frac{1}{2}$ (short dashed); (iii) $c = 1$; (iv) $c = \frac{3}{2}$. The unperturbed profile, $d(\xi) = 1$ is also shown in (b) (solid line).

bottom of the plane slope. However, its effect on the reflected amplitude is negligible. As the values of c increase, the protrusion is mapped further up the slope to the point where for $c = \frac{3}{2}$ it has the effect of rounding off the sharp join at the top of the slope. The variation in $|R_0|$ is now more pronounced and, although the modification to the original Booij bed profile is relatively small, the slight reduction in the minimum value of $h(x)$ is evidently significant.

5. Conclusions

The reflection and transmission of surface waves by varying topography has been considered by means of a conformal mapping technique originally devised by Fitz-Gerald (1976) and subsequently used by Evans & Linton (1994). When the two-dimensional fluid domain is mapped into a strip of constant width, the variable topography manifests itself in a variable coefficient in the transformed free-surface

condition which is much more slowly varying than the function defining the original bed, itself mapped to the lower boundary of the rectangular strip. The property of slow variations in the free-surface coefficient is exploited by using a variational principle as the basis of an approximation in the spirit of that used by Chamberlain & Porter (1995) (for example) to derive the modified mild-slope equation, in which the unknown function assumes a prescribed separable depth component. The combined effect of satisfying the bottom condition exactly, an advantage not enjoyed by the traditional mild-slope approximations, and dealing with a more slowly varying free-surface condition has allowed us to derive highly effective and straightforward approximations to wave scattering by variable beds of unrestricted slope.

Of course the difficult task of solving the original problem has not suddenly been overcome, but it has been considerably assisted by the fact that the mapping itself contributes significantly towards the solution. It is therefore of no surprise that the most demanding practical aspect is the derivation of the mapping function for any given bed profile, even though only the derivative of this function is required to approximate the scattering properties. Mapping functions which correspond to a number of families of bed profiles have been described in this paper as a means of illustrating the accuracy of the approximation and, of course, the range of examples could have been extended indefinitely. For instance, a family of bed profiles not included by Fitz-Gerald (1976) with $h_0 = h_1$ which represent, for $\beta = 1$, a symmetric triangular protrusion whose sloping sides make internal angles $\alpha \in (0, \frac{1}{2}\pi]$ with the x-axis, is defined by

$$F'(\zeta) = \left[\frac{(1 + e^{\beta\pi\zeta})}{(1 + \mu e^{\beta\pi\zeta})(1 + \mu^{-1}e^{\beta\pi\zeta})} \right]^{\pi/\alpha},$$

where $\mu \in (0, \infty)$ is a parameter which implicitly determines the height of the protrusion. Choosing values of $\beta < 1$ introduces a smoothing of the triangular profile.

However, for a particular bed shape the chance of knowing, or being able to derive, the exact mapping function is small, whilst the essence of the method is lost if the mapping is constructed by computational methods (some of which are suggested in the concluding remarks of Evans & Linton 1994). As a means of addressing this shortcoming, in §4 we have described an extension to the main method of the paper which allows for additional slowly varying perturbations of a fairly general form about a bed for which a mapping is assumed known. In this generalization, the basic principles that underpin the success of the original method are retained, and consequently so is the structure and simplicity of the resulting formulation.

One significant outcome of the present contribution that sets it apart from the vast body of previous work on this subject is that we are able to provide an accurate approximation to the reflected wave amplitude for variable topography in the form of an explicit expression. This comes from the truncation of the infinite series defining the analytic solution in §3.2 to just a single term and with $e(s)$ assumed to be small enough to be neglected. To summarize this result expressed in its simplest form, we have

$$|R_0| \approx 1/\sqrt{1 + |X|^{-2}}$$

where

$$X = \int_{-\infty}^{\infty} \left(\frac{\kappa'}{2\kappa} \right) \exp\left\{ -2\mathrm{i}\widehat{\kappa}s - 2\mathrm{i} \int_0^s (\kappa(t) - \widehat{\kappa}) \, \mathrm{d}t \right\} \mathrm{d}s, \qquad \widehat{\kappa} = \begin{cases} \kappa_0, & s < 0, \\ \kappa_1, & s > 0. \end{cases}$$

Here $\kappa' = [(1 + \cosh 2\kappa)/(2\kappa + \sinh 2\kappa)]f'$ whilst $f(s) = \kappa(s)\tanh\kappa(s)$ with κ_0, κ_1 denoting the asymptotic values of $\kappa(s)$ as $s \to \mp\infty$. The reader is referred to the discussion in §3.3 for an assessment of the accuracy of this formula. Despite it being the crudest of the approximations based on the present method we confidently expect it to outperform any of the traditional one-term mild-slope equations in terms of accuracy and the range of bed profiles to which it can be applied.

REFERENCES

ATHANASSOULIS, G. A. & BELIBASSAKIS, K. A. 1999 A consistent coupled-mode theory for the propagation of small-amplitude water waves over variable bathymetry regions. *J. Fluid Mech.* **389**, 275–301.

BENDER, C. J. & DEAN, R. G. 2003 Wave transformation by two-dimensional bathymetric anomalies with sloped transitions. *Coastal Engng* **50**, 61–84.

BERKHOFF, J. C. W. 1976 Mathematical models for simple harmonic linear waves. Wave diffraction and refraction. *Delft Hydr. Rep.* W 154-IV.

BOOIJ, N. 1983 A note on the accuracy of the mild-slope equation. *Coastal Engng* **7**, 191–203.

CHAMBERLAIN, P. G. & PORTER, D. 1995 The modified mild-slope equation. *J. Fluid Mech.* **291**, 393–407.

CHAMBERLAIN, P. G. & PORTER, D. 2006 Multi-mode approximations to wave scattering by an uneven bed. *J. Fluid Mech.* **556**, 421–441.

EVANS, D. V. 1985 The solution of a class of boundary-value problems with smoothly varying boundary conditions. *Q. J. Mech. Appl. Maths* **38**, 521–536.

EVANS, D. V. & LINTON, C. M. 1994 On step approximations for water wave problems. *J. Fluid Mech.* **278**, 229–249.

FITZ-GERALD, G. F. 1976 The reflexion of plane gravity waves travelling in water of variable depth. *Phil. Trans. R. Soc. Lond.* **34**, 49–89.

HAMILTON, J. 1977 Differential equations for long-period gravity waves on fluid of rapidly varying depth. *J. Fluid Mech.* **83**, 289–310.

KREISEL, G. 1949 Surface waves. *Q. Appl. Maths* **7**, 21–44.

MASSEL, S. R. 1993 Extended refraction-diffraction equation for surface waves. *Coastal Engng* **19**, 97–126.

MEI, C. C. 1983 *The Applied Dynamics of Ocean Surface Waves.* Wiley.

PORTER, D. 2003 The mild-slope equations. *J. Fluid Mech.* **494**, 51–63.

PORTER, D. & CHAMBERLAIN, P. G. 1997 Linear wave scattering by two-dimensional topography. In *Gravity Waves in Water of Finite Depth* (ed. J. N. Hunt), pp. 13–53. Computational Mechanics, Southampton.

PORTER, D. & STAZIKER, D. J. 1995 Extensions of the mild-slope equation. *J. Fluid Mech.* **300**, 367–382.

PORTER, D. & STIRLING, D. S. G. 1990 *Integral Equations.* Cambridge University Press.

PORTER, R. 1995 Complementary methods and bounds in linear water waves. PhD Thesis, University of Bristol, UK.

PORTER, R. & EVANS, D. V. 1995 Complementary approximations to wave scattering by vertical barriers *J. Fluid Mech.* **294**, 155–180.

PORTER, R. & PORTER, D. 2000 Water wave scattering by a step of arbitrary profile. *J. Fluid Mech.* **411**, 131–164.

ROSEAU, M. 1976 *Asymptotic Wave Theory.* North-Holland.

SMITH, R. & SPRINKS, T. 1975 Scattering of surface waves by a conical island. *J. Fluid Mech.* **72**, 373–384.

WEITZ, M. & KELLER, J. B. 1950 Reflection of water waves from floating ice in water of finite depth. *Commun. Pure Appl. Maths* **3**, 581–607.